Eur. Phys. J. B (2018) 91: 105
https://doi.org/10.1140/epjb/e2018-90109-6

THE EUROPEAN PHYSICAL JOURNAL B

Regular Article

About the relation of electron–electron interaction potentials with exchange and correlation functionals*

Adrián Gómez Pueyo[1] and Alberto Castro[1,2,a]

[1] Institute for Biocomputation and Physics of Complex Systems, University of Zaragoza, Calle Mariano Esquillor, 50018 Zaragoza, Spain
[2] ARAID Foundation, Av. de Ranillas 1-D, 50018 Zaragoza, Spain

Received 1 March 2018 / Received in final form 13 April 2018
Published online 6 June 2018

Abstract. We investigate, numerically, the possibility of associating to each approximation to the exchange-and-correlation functional in density-functional theory (DFT), an optimal electron–electron interaction potential for which it performs best. The fundamental theorems of density-functional theory (DFT) make no assumption about the precise form of the electron–electron interaction: to each possible electron–electron interaction corresponds an exchange-and-correlation functional. This fact suggests the opposite question: given some functional of the density, is there any electron–electron interaction for which it is the exact exchange-and-correlation functional? And, if not, what is the interaction for which the functional produces the best results? Within the context of lattice DFT, we study these questions by working on the one-dimensional Hubbard chain. The idea of associating an optimal interaction potential to each approximation to the exchange and correlation functionals suggests, finally, a procedure to optimise parameterised families of functionals: find that one whose associated interaction most closely resembles the real one.

1 Introduction

Density-functional theory [1,2] has become the most used electronic structure method, both in chemistry, materials science, or condensed matter physics. Many useful material properties can be accurately predicted with DFT calculations, at a fraction of the cost that any other comparable quantum chemistry theory would require. These properties include total energies, elastic constants, phonon dispersions, heat capacities, diffusion coefficients, thermal expansion coefficients, infrared spectra, etc. Extensions of DFT such as time-dependent DFT [3–5] can be used to reach properties that "pure" DFT cannot reach, such as electronic excitations.

Yet it is still an approximate method: even with unlimited time and computational resources, it cannot yield exact results. There are many systems and properties for which the approximate DFT results are not good enough [6,7]. Hundreds of approximations to the exchange and correlation functional (XCF) [8], the key unknown object, have been proposed over the last decades. None of them entirely satisfactory, due to the fundamentally hard nature of the problem [9]. It is therefore of the maximum relevance to investigate the theoretical nature of this elusive object.

In this article, we report a numerical investigation on the relationship between XCFs and electron–electron interaction potential functions (IFs). Although, in a non-relativistic setup this function is always the $1/r$ Coulomb interaction, the DFT can be formulated for generic functions: each choice produces an XCF. One may then ask the inverse question: is there any IF for which a given density functional X is the exact XCF? And if no IF exists that makes X exact, which is the *optimal* one, meaning that the DFT calculations computed with X are as close as possible to the exact results? This question associates an optimal IF to each approximate XCF. As we shall see, this association naturally suggests a numerical procedure to optimise, ab initio, parameterised families of XCFs: find the particular XCF, within a family, whose associated IF most closely resembles the real IF.

We have started this research with the numerically tractable setup of site-occupation DFT, also frequently known as lattice DFT [10–12]. We consider the version of the theory based on the density only, i.e. the diagonal of the one-particle density-matrix, and not on the full matrix as it is sometimes considered [13–15] (in fact, as shown by Schönhammer et al. [12], other DFTs based on other variables are also possible). Lattice models (Anderson, Pariser–Parr–Pople, Heisenberg, Hubbard, etc.) have been extensively used, for example for the study

* Contribution to the Topical Issue "Special issue in honor of Hardy Gross", edited by C.A. Ullrich, F.M.S. Nogueira, A. Rubio, and M.A.L. Marques.

[a] e-mail: acastro@bifi.es

of strongly correlated many-electron systems. The use of these limited size lattice systems permits to carefully control the number of degrees of freedom of the investigated objects. Moreover, they can also be regarded as numerical discretisations of the real continuous three-dimensional models – that can be obtained in the limit of infinitely fine discretisation.

In particular, we have restricted our calculations to the one-dimensional Hubbard model (1DHM) [16–18]. For the choice of XCF, we have looked at the local density approximation, as parameterised by Lima et al. [19], using the exact results provided by the Bethe ansatz [20] solution [21]. It is the analogous to the usual LDA for the 3D homogeneous electron gas. This functional is entirely determined by the IF, which in the 1DHM is given by a single parameter. In this way, we have a one-parameter family of XCFs. Interestingly, the application of the optimisation procedure mentioned above leads, as we will show, to an optimal XCF whose interaction parameter does not correspond with the one used for the exact calculations. In other words, the best possible BALDA is not the one whose defining interaction parameter is the real one that defines the original many-electron problem.

The following section clarifies the previously outlined ideas; results are presented in Section 3, and the article concludes in Section 4.

2 Method

DFT addresses the N-electron problem whose Hamiltonian has usually the form:

$$\hat{H} = \sum_{\sigma} \int \mathrm{d}^3 r\ \hat{\psi}^{\dagger}_{\sigma}(\mathbf{r}) \left[-\frac{\nabla^2}{2} \right] \hat{\psi}_{\sigma}(\mathbf{r}) + \int \mathrm{d}^3 r\ v(\mathbf{r}) \hat{n}(\mathbf{r}) + \frac{1}{2} \sum_{\sigma\tau} \int \mathrm{d}^3 r \int \mathrm{d}^3 r'\ w(|\mathbf{r} - \mathbf{r}'|) \hat{\psi}^{\dagger}_{\sigma}(\mathbf{r}) \hat{\psi}^{\dagger}_{\tau}(\mathbf{r}') \times \hat{\psi}_{\tau}(\mathbf{r}') \hat{\psi}_{\sigma}(\mathbf{r}). \quad (1)$$

The pair $\hat{\psi}^{\dagger}_{\sigma}(\mathbf{r}), \hat{\psi}_{\sigma}(\mathbf{r})$ are the creation/annihilation field operators at position $\mathbf{r}$ and spin projection σ, and $\hat{n}(\mathbf{r}) = \sum_{\sigma} \hat{\psi}^{\dagger}_{\sigma}(\mathbf{r}) \hat{\psi}^{\dagger}_{\sigma}(\mathbf{r})$ is the density operator. The first term in equation (1) is the kinetic operator $\hat{T}$, whereas the second term is the external potential $\hat{V}$, fully determined by a local (in real space) function v. The last term is the two-electron interaction $\hat{W}$, also characterised by a local function w, dependent on the distance between any pair of electrons; normally this is simply the Coulomb function: $w(r) = 1/r$.

However, the fundamental theorems of DFT make no use of the particular form of function w, and could be formulated for any other interaction function (IF) – although some restrictions must exist, to ensure that the Hamiltonian has a lower bound, for example. We may represent all *admissible* IFs in a manifold Γ, so that to each $\gamma \in \Gamma$ corresponds a w^{γ}. Once we fix a given γ, the DFT theorems ensure the existence of an exchange-and-correlation functional (XCF) of the one-electron density n, $E^{\gamma}_{\mathrm{xc}} = E^{\gamma}_{\mathrm{xc}}(n)$. This object may then be used, thanks to the resolution of the Kohn–Sham [22] auxiliary non-interacting electron problem, for the prediction of the ground-state energy and density – and with it, in principle, of any ground-state observable.

We have therefore defined a map from Γ to a set Λ, a manifold whose elements represent candidates to XCFs:

$$l : \Gamma \to \Lambda \qquad \gamma \to l(\gamma) = \lambda. \quad (2)$$

It assigns an XCF functional represented by λ to the IF γ. One may then wonder about the possible inverse map: given a functional of the density that we can use as XCF, is there any IF for which it is the exact XCF? This question may be asked of any of the approximate XCFs currently in use: they are not exact for the Coulomb interaction, but could they be exact for any other IF? Such kind of questions, in the DFT literature, are usually called "representability problems", although representability is normally predicated of densities and external potentials, not of density functionals and interaction potentials.

Although finding out the theoretical conditions for a density functional to be the exact XCF of some IF may be an interesting problem itself, in this work we have merely followed a numerical, practical route to the problem, namely an optimisation procedure. Let us now consider that the rather abstract objects Γ and Λ above are parameter sets that determine the form of IFs and XCFs, respectively. Given a functional $E^{\lambda}_{\mathrm{xc}}$ and an IF γ, we define:

- the exact ground state density $n_{\gamma}[v]$ corresponding to some external potential v, and
- the DFT ground state density $n^{\mathrm{DFT}}_{\lambda}[v]$, computed by solving the Kohn–Sham's equations with the XCF λ.

λ is the exact XCF corresponding to γ (i.e. $\gamma \in l^{-1}(\lambda)$) if and only if both densities coincide for any choice or v. Otherwise, we may define, for some set of external potentials $\{v_k\}$, a function of γ given by the distance between the two densities:

$$G(\gamma; \lambda, \{v_k\}) = \sum_k \int \mathrm{d}^3 r\ (n_{\gamma}[v_k](\mathbf{r}) - n^{\mathrm{DFT}}_{\lambda}[v_k](\mathbf{r}))^2. \quad (3)$$

If $\gamma_0 \in l^{-1}(\lambda)$, then G attains its minimum value at zero. Inversely, however, given a minimum γ_0 of G, even if it yields zero, one cannot guarantee that λ is its corresponding XCF, as the set of external potentials does not include them all. Nevertheless, it is in some sense the *optimal* IF for the given XCF λ, as their corresponding exact and DFT densities are the ones that most closely resemble each other.

In this way, we have defined a function $\gamma^{\min}(\lambda)$ that associates to each functional an IF $\gamma = \gamma^{\min}(\lambda)$:

$$G(\gamma^{\min}(\lambda); \lambda, \{v_k\}) = \min_{\gamma \in \Gamma} G(\gamma; \lambda, \{v_k\}). \quad (4)$$

If this minimum is actually zero, and the external potentials set is a sufficiently good sample, we may be assured

that the functional is a very good approximate XCF for the its corresponding IF.

We therefore have a procedure that may be used as a measure of the "quality" of a given approximated XCF, by answering two questions: (1) does it actually correspond to some IF, i.e. is it the exact XCF for some IF? This question can of course be only answered approximately, by looking at how much the minimum value approaches zero. (2) How much does its associated IF resemble the true electron–electron interaction?

The formulation of these two questions immediately suggests a procedure to find the optimal XCF in the given family Λ: given two IFs γ_1 and γ_2, a distance between them may be simply defined as:

$$d(\gamma_1,\gamma_2) = \left(\int_0^\infty \mathrm{d}r\ (w^{\gamma_1}(r) - w^{\gamma_2}(r))^2\right)^{1/2}. \quad (5)$$

If γ_{ref} represents the true IF, then the minimisation of the function

$$H(\lambda) = d^2(\gamma_{\mathrm{ref}}, \gamma^{\min}(\lambda)), \quad (6)$$

leads to an XCF λ_0 whose associated IF is as close as possible to the reference IF γ_{ref}.

We have first attempted these ideas on the lattice or "site-occupation" version of DFT, that substitute the continuous creation and annihilation field operators in equation (1) by a discrete set $\hat{d}^\dagger_{m\sigma}, \hat{d}_{m\sigma}$, corresponding to a basis localised around a finite number of "sites". Furthermore, if we restrict the IF to only on-site interactions, and the kinetic term to couple only nearest neighbours in a one-dimensional chain, we end up with the one-dimensional Hubbard model (1DHM) [16–18]:

$$\hat{H} = -t\sum_{\langle m,n\rangle\sigma} \hat{d}^\dagger_{m\sigma}\hat{d}_{n\sigma} + \sum_n v_n\hat{n}_n + U_{\mathrm{ee}}\sum_n \hat{n}_{n\uparrow}\hat{n}_{n\downarrow}, \quad (7)$$

where $\langle m,n\rangle$ denotes summation over nearest neighbours only. The kinetic term may couple the two extreme sites of the chain (periodic boundary conditions, PBC) or not (open boundary conditions, OBC). Note that both the kinetic and interaction operators are determined by a single constant (t and U_{ee}, respectively), implying homogeneous couplings along the chain – this condition could be relaxed. In the following, we will fix the unit of energy by setting $t = 1$.

The KS formulation of DFT attacks this many-electron problem by means of the solution of the KS equations:

$$\sum_n \left[t_{mn} + \delta_{mn}(v_m + v_m^{\mathrm{Hxc}(\lambda)}(n))\right]\varphi^\alpha_{n\sigma} = \varepsilon^\alpha\varphi^\alpha_{m\sigma}, \quad (8)$$

for $\sigma = \uparrow,\downarrow$ and $\alpha = 1,\ldots,N$ (the number of electrons), and $t_{mn} = -t(\delta_{m,n+1} + \delta_{m,n-1})$. The density is given by:

$$n_m = \sum_{\alpha\sigma} |\varphi^\alpha_{m\sigma}|^2. \quad (9)$$

It determines the form of the Hartree, exchange and correlation potential, given by the derivative of an energy density function(al):

$$v_m^{\mathrm{Hxc}(\lambda)}(n) = \frac{\partial E^\lambda_{\mathrm{Hxc}}}{\partial n_m}(n), \quad (10)$$

for which some approximation must be used. Typically, one separates a Hartree part, and uses approximations for the remaining exchange and correlation. However, in this work we have focused on a case where the full Hxc energy is approximated directly: the local density-approximation (LDA) for the 1DHM, known as Bethe ansatz [20] LDA (BALDA), since it is based on the Bethe ansatz solution for the homogeneous infinite chain Hubbard system. It was worked out by Lieb and Wu [21], and a parameterisation to this solution was provided in reference [19]: the total energy per site for an infinite homogeneous 1DHM with interaction constant U and constant density $\tilde{n}$ ($\tilde{n} \le 1$) is given by:

$$\varepsilon^{\mathrm{hom}}_<(\tilde{n},U) = -\frac{2\beta(U)}{\pi}\sin\left(\frac{\pi\tilde{n}}{\beta(U)}\right). \quad (11)$$

The function $\beta(U)$ is the solution to:

$$-\frac{2\beta(U)}{\pi}\sin\left(\frac{\pi}{\beta(U)}\right) = -4\int_0^\infty \mathrm{d}x \frac{J_0(x)J_1(x)}{x[1+\exp(Ux/2)]}, \quad (12)$$

where J_0 and J_1 are the zero-th and first order Bessel functions. For $n \ge 1$, the application of particle–hole symmetry implies [21]:

$$\varepsilon^{\mathrm{hom}}_>(\tilde{n},U) = (\tilde{n}-1)U + \varepsilon^{\mathrm{hom}}_<(2-\tilde{n},U), \quad (13)$$

so that, for all $\tilde{n}$,

$$\begin{aligned}\varepsilon^{\mathrm{hom}}(\tilde{n},U) = {}& \theta(1-\tilde{n})\varepsilon^{\mathrm{hom}}_<(\tilde{n},U) \\ & +\theta(\tilde{n}-1)\varepsilon^{\mathrm{hom}}_>(\tilde{n},U),\end{aligned} \quad (14)$$

where θ is the Heaviside function. This expression has a cusp at $n = 1$, making the derivative (needed to determine the KS potential) discontinuous. This fact has been used to compute the Mott gap [23], but it is also a problem, as: (1) the KS calculation are difficult to converge due to the presence of the discontinuity: in our case we have used the addition of a smoothing function as suggested by Kurth et al. [24]; (2) the exact functional has no such cusp (this fact proved to be crucial in our calculations for the Hubbard dimer, as shown below).

The total energy (per unit cell, if PBC are used) is then given by:

$$E^{\mathrm{hom}}(n,U) = \sum_n \varepsilon^{\mathrm{hom}}(n_n,U). \quad (15)$$

The Hartree plus exchange and correlation energy functional is then defined by subtracting the non-interacting from the interacting total energy:

$$E_{\mathrm{Hxc}}^{\mathrm{BALDA}(U)}(n,U) = E^{\mathrm{hom}}(n,U) - E^{\mathrm{hom}}(n,0). \quad (16)$$

We have therefore defined a one parameter family of XCFs: in this case, $\lambda \equiv U$, i.e. the parameter is the interaction constant U. We will hereafter use the notation $G(U_{ee}; U, \{v_k\})$ for the function defined in equation (3), $U_{ee}^{min}(U)$ for the function that provides the minimum in equation (4), and $H(U)$ for the function defined in equation (6).

In the following section, we will show the results for the optimisation procedure described above: first, the computation of function G given, in the lattice case, by:

$$G(U_{ee}; U, \{v_k\}) = \sum_k \sum_m (n_{U_{ee}}[v_k]_m - n_U^{DFT}[v_k]_m)^2. \quad (17)$$

Then, we performed the minimisation of this function in order to build the function $U_{ee}^{min}(U)$ that provides the optimal interaction constant U_{ee} for a given BALDA constant U. Finally, the minimisation of the function $H(U)$ yields the optimal BALDA constant, in the sense that its associated optimal interaction constant is as close as possible to a previously defined reference one.

3 Results

The first step of the program outlined above is the computation of function $G(U_{ee}; U, \{v_k\})$ for varying values of U_{ee}, U, and a random set of external potentials. In Figure 1 we display this function for lattices with 2 (top), 8 (middle) and 14 (bottom) sites. In all cases, we populated the lattices with two electrons. We explore values of $U \in [0, 1]$. This implies the regime of weak interaction (for example, the correlation for $U = 0.5$ is approximately 0.2% of the total energy for the 8 sites case). We used 10 external random-generated potentials to build the set $\{v_k\}$; we found that this number was enough to find converged solutions for the minimisations described below. The potentials are small perturbations (they are generated by taking a flat random distribution of potential values in the interval $[0, 0.01t]$), and in consequence we are exploring densities that do not deviate much from the ground-state solution with $v = 0$.

Then, for each U, we sought for the minimum of G as a function of U_{ee}. For that purpose, we have chosen a gradient-based algorithm [25,26]. The gradient of G with respect to U_{ee} is given by:

$$\frac{\partial G}{\partial U_{ee}} = \sum_k \sum_m 2(n_{U_{ee}}[v_k]_m - n_U^{DFT}[v_k]_m) \frac{\partial}{\partial U_{ee}} n_{U_{ee}}[v_k]_m, \quad (18)$$

and

$$\frac{\partial}{\partial U_{ee}} n_{U_{ee}}[v_k]_m = 2\mathrm{Re}\langle \Psi^k | \hat{n}_m | \frac{\partial \Psi^k}{\partial U_{ee}} \rangle, \quad (19)$$

where $\Psi^k = \Psi^k(U_{ee})$ is the ground state of the system corresponding to the v_k external potential for some U_{ee} electron–electron interaction parameter. The problem therefore boils down to the computation of the derivatives of Ψ^k, which may be done by making use of Sternheimer's equation:

$$\left[\hat{H} - E_k\right] | \frac{\partial \Psi^k}{\partial U_{ee}} \rangle = -[\hat{I} - |\Psi^k\rangle\langle\Psi^k|] \sum_m \hat{n}_{m\uparrow}\hat{n}_{m\downarrow}|\Psi^k\rangle, \quad (20)$$

where E_k is the ground state energy corresponding to the external potential v_k.

The found minima form a curve $U_{ee}^{min}(U)$, also shown in Figure 1 in red for the three lattices. It can be seen how these curves are not straight lines $U_{ee}^{min}(U) = U$ following the diagonal of the xy plane. This means that the electron–electron interaction U_{ee} that produces the closest densities to the ones produced by BALDA calculations with a parameter U is in fact different from U. This effect seems to grow with the number of sites, and also with increasing U (we have performed calculations up to 22 sites).

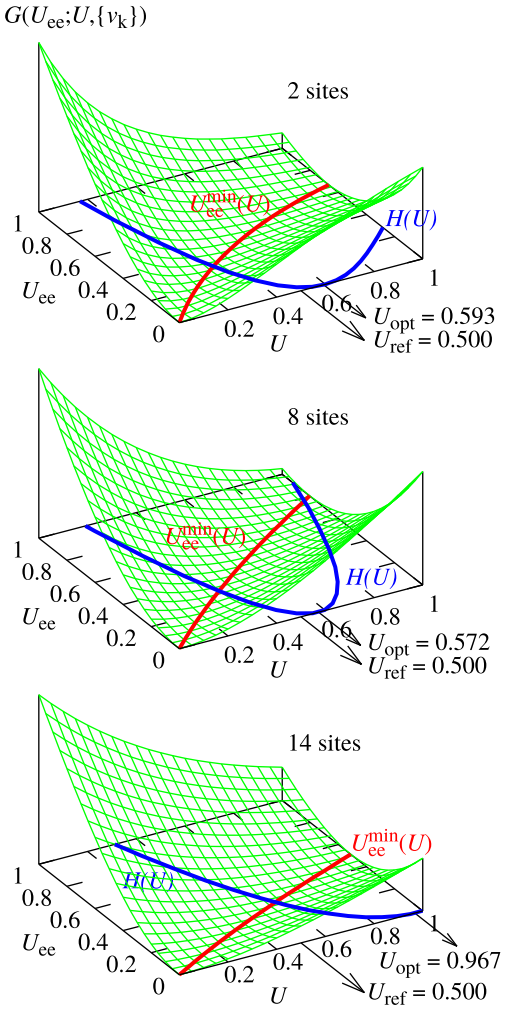

Fig. 1. Function $G(U_{ee}, U; \{v_k\})$ (surfaces) for a lattice with 2 (top), 8 (middle), and 14 (bottom) sites. The curve determined by the minima of this function with respect to U_{ee}, i.e. U_{ee}^{min} is overlaid on the surface (in red). Function $H(U)$ is also plotted on the xy plane (in blue). Finally, the reference U_{ref}, and the optimised BALDA parameter, U_{opt} [at the minimum of function $H(U)$], are also marked.

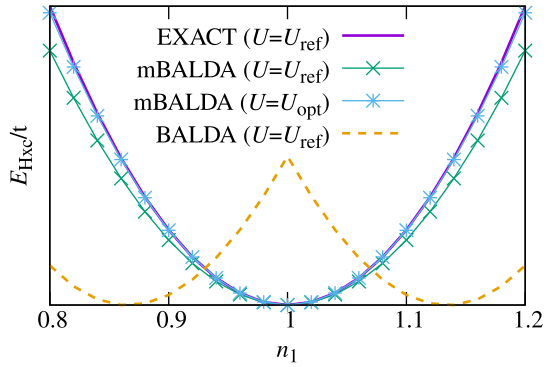

Fig. 2. Functional $E_{\rm Hxc}$ (the sum of the Hartree and xc correlation energies), as a function of the density n_1 of one of the sites of a Hubbard dimer. The plot displays the exact and BALDA functional computed with the $U_{\rm ee}^{\rm ref}$ interaction (EXACT), and the mBALDA functional (see text its definition) computed with the same reference $U_{\rm ee}^{\rm ref}$ and with the optimised $U_{\rm opt}$.

Therefore, we have associated an electron–electron interaction $U_{\rm ee}$ to each member of our one-parameter family of xc functionals. We wish now to find the member of that family whose associated electron–electron interaction most closely resembles a reference one. We set this reference electron–electron interaction parameter to $U_{\rm ee}^{\rm ref} = 1/2$. Then, we minimise function $H(U)$, defined as:

$$H(U) = (U_{\rm ee}^{\rm ref} - U_{\rm ee}^{\rm min}(U))^2. \tag{21}$$

The minimum is the optimal value $U_{\rm opt}$ for the BALDA functional for a given electron–electron interaction parameter $U_{\rm ee}^{\rm ref}$.

As we can see again in Figure 1, the obtained $U_{\rm opt}$ differs substantially from the reference $U_{\rm ee}^{\rm ref}$. The optimal value also depends on the number of sites N_s, and we observed that it grows with it for any $N_s > 2$. Therefore, we see that for a given reference electron–electron interaction $U_{\rm ee}$, the *optimal* BALDA is not the one defined with that parameter, but there exists an optimal $U_{\rm opt}$ that minimises the error in the results.

The two-sites case is however special: in fact $U_{\rm opt}$ for two sites is larger than for eight sites. It is not surprising, since we have treated this case differently: we have not used the "real" BALDA functional that treats differently the $n > 1$ and $n < 1$ cases, but rather we have used equation (11) also for $n > 1$. In fact, if one uses the real BALDA functional for the Hubbard dimer, the optimisation procedure finds $U_{\rm ee}(U) = 0$ and $U_{\rm opt} = 0$. In other words, the best possible BALDA functional is the zero functional, and inversely, for a given BALDA functional the best possible Hubbard electron–electron interaction constant is zero. The reason is that, for the range of densities we are exploring (n_1 and n_2 both close to 1), the BALDA functional for the Hubbard dimer is a very bad approximation due to the presence of the discontinuity.

This fact can be understood by looking at Figure 2. This figure also serves the purpose of showing how the optimisation procedure produces a functional that closely resembles the exact one, at least for the densities region explored by the set of external potentials used in the definition of function G. The plot shows the $E_{\rm Hxc}$ functionals for the 2-site model as a function of the density in site one n_1 (obviously, $n_2 = 2 - n_1$): the exact functional (for details about the computation of the exact functional, see Appendix A), the BALDA functional computed with the reference U, and the "modified" BALDA functional (mBALDA) that uses the energy expression that is only valid for $n < 1$ for the whole range of densities, both with the reference U and with the optimised one, $U_{\rm opt}$.

The optimised mBALDA functional produces a very good approximation to the exact $E_{\rm Hxc}$, at least for the range of densities typically sampled by the random set of potentials. It can be seen how it improves over the original functional defined with the "real" interaction constant $U_{\rm ee}^{\rm ref}$. The plot also shows the reason behind the failure of the real BALDA functional: the cusp at $n = 1$. As discussed in reference [27], in this regime of weak interaction, and specially near half filling (as it is the case for the dimer), the parametrization is very wrong. The discontinuity, as also shown in our figure, has even the wrong sign (the value at $n = 1$ is a maximum instead of a minimum as it is for the exact functional). It is clear how, in this region, the best possible way to approximate this curve to the exact one is by making this cusp disappear. The cusp height depends on U, and only disappears for $U = 0$, at which point the functional also vanishes. This makes the BALDA family of functionals impractical for our optimisation procedure in the Hubbard dimer case. In all other cases, however, we have used the normal BALDA family of functionals, and found similarly good optimised approximations to the exact functional

4 Conclusions

We have defined a procedure to associate, numerically, an electron–electron interaction function (IF) to each approximation of the exchange-and-correlation functional (XCF) of DFT. It is defined as the IF for which the XCF performs best. It is, in general, not the real IF (the Coulomb interaction function for electrons in 3D). We have performed a first study in this direction by working with lattice DFT models – in particular the Hubbard chain, since it allows to work with a reduced number of degrees of freedom. By employing the local density-approximation (LDA) for Hubbard chains, we could observe how the Hubbard interaction constant that best matches the LDA functional is not the one used to define the functional.

This association process immediately defines a procedure to optimise parameterised families of XCFs: search for the one whose associated IF most closely resembles the real IF. Adjusting a number of parameters in the definition of the XCF in order to optimise its performance has often been used as a method to produce new and better functionals. Often, the optimisation focused on the ground-state energies, for a given set of external potentials, as the basis of comparison. However, it has been pointed out that this may not be the best option [28].

A different option is to look at the densities. This is the approach taken, for example, in reference [29], that also considers one-dimensional lattice models to investigate the possibility of adjusting *ansatze* for the XCF. Our work builds on this idea, but focuses on a smaller object for the comparison: the associated IF, rather than the full set of densities for the sample set of external potentials.

The transition to the first principles 3D case will permit to answer interesting questions: what are the associated IFs for the typical 3D XCF in use? Is the 3D LDA associated IF more or less short-ranged than the Coulomb interaction? Is it screened? How does the correction of its asymptotic behaviour affect the associated IF? What about the IF associated to more sophisticated (gradient-corrected/hybrid functionals, etc.)? However, it remains to be seen how the concept can be scaled. By working with the 1DHM and the LDA, the number of degrees of freedom defining the IF is reduced to one, and the number of parameters defining the family of XCFs is also only one. The optimisation searches will grow in complexity if we increase the number of degrees of freedom for those objects. Also, the procedure requires the computation of exact, or at least high quality densities. Therefore the transition from one-dimensional lattice models to the full three-dimensional ab-initio description of molecules and solids will be a challenging computational problem.

AC is indebted, first and foremost, to Hardy Gross, for whom he had the opportunity of working for five productive years. It was with Hardy with whom I finally understood (partially) the intricate subtleties of density-functional theory. Working at his group was an eye-opening learning experience.

We acknowledge support from the Ministerio de Economía y Competitividad (MINECO) grants FIS2013-46159-C3-2P, FIS2017-82426-P and FIS2014-61301-EXP.

Author contribution statement

All the authors were involved in the preparation of the manuscript. All the authors have read and approved the final manuscript.

Appendix A: Computation of the exact Hxc functional

The exact Hxc functional is defined as:

$$E_{\mathrm{Hxc}}(n) = F(n) - T_{\mathrm{S}}(n), \tag{A.1}$$

where

$$F(n) = \min_{\Psi \in M(n)} \langle \Psi | (\hat{T} + \hat{W}) | \Psi \rangle, \tag{A.2}$$

$$T_{\mathrm{S}}(n) = \min_{\Psi \in M(n)} \langle \Psi | \hat{T} | \Psi \rangle. \tag{A.3}$$

The set $M(n)$ contains all the wave functions whose density is n. In principle, one could compute these objects in a straightforward approach by performing the minimisation over $\Psi \in M(n)$. However, it is more efficient to do a "density-to-potential inversion" [30]; in our case we have used the following procedure:

The functional F is universal, inasmuch as it does not depend on any external potential. One may however define a potential-dependent functional:

$$E(n) = F(n) + \sum_m v_m n_m,$$

for some external potential $v \equiv \{v_m\}$. If it is the potential whose ground-state density is n, then $E(n)$ is the ground state energy, and one can compute $F(n)$ using the previous formula. Therefore, one needs to compute the potential whose ground state density is n, which can be done through the minimisation of the function:

$$K(v) = \sum_m (n(v)_m - n_m)^2, \tag{A.4}$$

where $n(v)$ is the ground-state density corresponding to v, computed by solving Schrödinger's equation. At the solution point, $K(v) = 0$, the two densities coincide and the map $n \to v$ has been achieved, which allows to compute $F(n)$ through equation (A.4). The same procedure can be used to compute $T_S(n)$.

The numerical minimisation procedure for K can be helped if we are able to compute the gradient of K, given by:

$$\frac{\partial K}{\partial v_n}(v) = \sum_m 2(n(v)_m - n_m) \frac{\partial}{\partial v_n} \langle \Psi(v) | \hat{n}_m | \Psi(v) \rangle, \tag{A.5}$$

where $\Psi(v)$ is the ground-state corresponding to the external potential v. It is obtained as the solution to Schrödinger's equation; its gradient $\frac{\partial}{\partial v_n}\Psi(v)$ can be obtained through the solution of Sternheimer's equation, using $\hat{n}_m$ as the perturbation:

$$\left[\hat{H} - E\right] | \frac{\partial \Psi}{\partial v_n} \rangle = -[\hat{I} - |\Psi(v)\rangle\langle\Psi(v)|] \hat{n}_m |\Psi(v)\rangle. \tag{A.6}$$

References

1. P. Hohenberg, W. Kohn, Phys. Rev. **136**, B864 (1964)
2. R.M. Dreizler, E.K.U. Gross, *Density functional theory: an approach to the quantum many-body problem* (Springer-Verlag, Berlin, Heidelberg, 1990)
3. E. Runge, E.K.U. Gross, Phys. Rev. Lett. **52**, 997 (1984)
4. M.A.L. Marques, N.T. Maitra, F.M.S. Nogueira, E.K.U. Gross, A. Rubio, eds., *Fundamentals of time-dependent density functional theory* (Springer-Verlag, Berlin-Heidelberg, 2012)
5. C.A. Ullrich, *Time-dependent density-functional theory: concepts and applications* (Oxford Scholarship, Oxford, 2011)
6. A.J. Cohen, P. Mori-Sánchez, W. Yang, Science **321**, 792 (2008)
7. K. Burke, J. Chem. Phys. **136**, 150901 (2012)
8. M.A. Marques, M.J. Oliveira, T. Burnus, Comput. Phys. Commun. **183**, 2272 (2012)

9. N. Schuch, F. Verstraete, Nat. Phys. **5**, 732 (2009)
10. O. Gunnarsson, K. Schönhammer, Phys. Rev. Lett. **56**, 1968 (1986)
11. A. Schindlmayr, R.W. Godby, Phys. Rev. B **51**, 10427 (1995)
12. K. Schönhammer, O. Gunnarsson, R.M. Noack, Phys. Rev. B **52**, 2504 (1995)
13. R. López-Sandoval, G.M. Pastor, Phys. Rev. B **61**, 1764 (2000)
14. W. Töws, G.M. Pastor, Phys. Rev. B **83**, 235101 (2011)
15. R. López-Sandoval, G.M. Pastor, Phys. Rev. B **69**, 085101 (2004)
16. E.H. Lieb, F. Wu, Physica A **321**, 1 (2003) [Statphys-Taiwan-2002: Lattice Models and Complex Systems]
17. K. Capelle, N.A. Lima, M.F. Silva, L.N. Oliveira, Density-functional theory for the Hubbard model: numerical results for the Luttinger liquid and the Mott insulator, in *The fundamentals of electron density, density matrix and density functional theory in atoms, molecules and the solid state*, edited by N.I. Gidopoulos, S. Wilson (Springer, Dordrecht, Netherlands, 2003), pp. 145–168
18. D.J. Carrascal, J. Ferrer, J.C. Smith, K. Burke, J. Phys.: Condens. Matter **27**, 393001 (2015)
19. N.A. Lima, M.F. Silva, L.N. Oliveira, K. Capelle, Phys. Rev. Lett. **90**, 146402 (2003)
20. H. Bethe, Zeitschrift für Physik **71**, 205 (1931)
21. E.H. Lieb, F.Y. Wu, Phys. Rev. Lett. **20**, 1445 (1968)
22. W. Kohn, L.J. Sham, Phys. Rev. **140**, A1133 (1965)
23. N.A. Lima, L.N. Oliveira, K. Capelle, Europhys. Lett. **60**, 601 (2002)
24. S. Kurth, G. Stefanucci, E. Khosravi, C. Verdozzi, E.K.U. Gross, Phys. Rev. Lett. **104**, 236801 (2010)
25. D. Kraft, ACM Trans. Math. Softw. **20**, 262 (1994)
26. S.G. Johnson, *The NLopt nonlinear-optimization package*, http://ab-initio.mit.edu/nlopt
27. V.V. França, D. Vieira, K. Capelle, New J. Phys. **14**, 073021 (2012)
28. M.G. Medvedev, I.S. Bushmarinov, J. Sun, J.P. Perdew, K.A. Lyssenko, Science **355**, 49 (2017)
29. M. Lubasch, J.I. Fuks, H. Appel, A. Rubio, J.I. Cirac, M.C. Bañuls, New J. Phys. **18**, 083039 (2016)
30. D.S. Jensen, A. Wasserman, Phys. Chem. Chem. Phys. **18**, 21079 (2016)